https://doi.org/10.33271/nvngu/2025-4/079

T. V. Kimstach[1,2],
orcid.org/0000-0002-8993-201X,
K. I. Uzlov[1],
orcid.org/0000-0003-0744-9890,
O. P. Bilyi[1],
orcid.org/0000-0003-1234-5404,
L. I. Solonenko[3],
orcid.org/0000-0003-2092-8044,
S. I. Repyakh[*1],
orcid.org/0000-0003-0203-4135

1 – Ukrainian State University of Science and Technologies, Dnipro, Ukraine
2 – Iron and Steel Institute of Z. I. Nekrasov National Academy of Sciences of Ukraine, Dnipro, Ukraine
3 – Odesa Polytechnic National University, Odesa, Ukraine
* Corresponding author e-mail: 123rs@ua.fm

DETERMINATION OF BRONZE БрА7К2О1,5Мц0,3 CRYSTALLIZATION INTERVAL LIMIT VALUES AND PHASE TRANSFORMATIONS

Phase transformations temperatures, crystallization intervals, etc. are any alloy's fundamental parameters. Alloys' casting, technological and operational properties are related to them. Nevertheless, unlike two-component bronzes, such requirements for multi-component structural, non-magnetic, corrosion-resistant bronze БрА7К2О1,5Мц0,3 are absent.

Purpose. For Cu-Al-Si-Sn-Mn system bronzes, crystallization intervals quantitative values (liquidus and solidus temperatures, crystallization interval size and solid phase relative share in it) have been established. БрА7К2О1,5Мц0,3 bronze's alloying components' synergistic and selective influence on its crystallization interval and relative fluidity indicators changing has been determined.

Methodology. Well-known methods and research techniques, including thermography, differential thermal analysis, spectral chemical analysis, images analysis digital method have been used in this work. Bronzes fluidity has been assessed using spiral test. Bronze's alloying elements' synergistic and selective influences on its characteristics have been determined using chemical elements ratio in it (K_R criterion) and experimental data results processing by Excel computer program.

Findings. In bronze БрА7К2О1,5Мц0,3 with K_R criterion value rising from 0.35 to 0.84, there increase liquidus, solidus temperatures and crystallization interval from 32 to 49 °C. Bronze's alloying elements' (Al, Si, Sn, Mn) synergistic and selective influences on its crystallization interval limit values have been determined. It has been established that conditionally-veritable fluidities of БрА7К3О1,5Мц0,3 and БрА9Ж3Л bronzes are practically the same. For Cu-Al-Si-Sn-Mn system bronzes with K_R = 0.35–2.07, solid phase relative volume fraction (φ_{SP}) in crystallization temperature range is 60–63 %.

Originality. For the first time, limiting values and phase transformations for БрА7К2О1,5Мц0,3 bronze's crystallization interval and alloying elements synergistic and selective influence on these indicators have been determined.

Practical value. Based on БрА7К2О1,5Мц0,3 bronze's chemical composition selected, mathematical models have been proposed for its liquidus and solidus temperatures calculating and for transition from dependences of solid phase $t(\varphi_{SP})$ volume fraction in crystallization temperature range to temperatures' absolute values $t(\varphi_{SP})$. Their use will allow increasing the indicators of foundry and technological parameters accuracy forecasting.

Keywords: *bronze, liquidus, solidus, crystallization interval, fluidity, temperature*

Introduction. At the present, structural, corrosion-resistant aluminum bronzes are one of the most acceptable materials in all industries, from mining to shipbuilding and aircraft construction. Nevertheless, this foundry bronzes class requires its own study in connection with technical evolution next stage development – multicomponent (complex alloyed) bronzes with specified preferential properties complexes applying. At the same time, among aluminum bronzes "basic" parameters, as well as any other casting alloys, perhaps the most important is crystallization temperature interval itself and the processes that accompany alloys solidification and their structure formation.

Processes occurring in alloys' crystallization temperature range (Δt_{LS}) during their solidification are the subject of many scientists and researchers works, including A. Bochvar (1952), N. Khvorinov (1956), B. Chalmers (1957), M. Flemings (1977), F. Kotlyarsky (1995, 2018), and others. Increased attention to this temperature range is due to the fact that any alloy casting and consumer properties largely depend on it.

Alloys' crystallization temperature interval is characterized not only by its absolute value, but also by its reference points – temperatures, including: liquidus (t_L) and solidus (t_S) temperatures, liquid residue pouring temperature (t_P) and variable composition melt filtration termination (t_T) temperature in alloy's two-phase state region during its crystallization. In addition to theoretical importance, all these crystallization temperature range reference points also have a purely practical significance. In particular, the value Δt_{LS} is calculated from the values t_L and t_S. Respectively, based on the fact that with value of Δt_{LS} increasing the tendency of the alloy to develop a columnar structure, hot cracks and gouging in castings decreases, the technological possibilities for manufacturing castings by various casting methods, casting molds, and casting nomenclature expand, but fluidity and obtaining cast parts with high tightness probability decrease. According to value Δt_{LS}

alloy casting processability and its suitability for cast parts with corresponding set of preferential properties manufacturing could be predicted. In foundries, such analysis result allows making rational technological decisions to avoid or prevent significant casting defects due to joints, under-casting, their surface waviness, hot cracks and others, to stabilize castings accuracy, to increase the yield of suitable parts, etc. [1, 2].

The value t_L determines alloy melt overheating temperature for its deoxidation technological implementation, modification, and pouring into foundry molds, melt thermo-temporal treatment mode for homogenization or its hereditary properties saving, etc. Values t_S determine maximum temperatures of casting heat treatment or castings hot isostatic pressing, etc. [3, 4].

Temperature t_P, in fact, is the temperature at which in alloy two-phase region during its crystallization upon undercooling below liquidus line, primary crystals, regularly arranged on their own singular nuclei in the melt, or interconnected dendrites framework formed, and the melt filtration process into the inter-branches space begins. This temperature is a key parameter in the manufacture of, for example, double-layer pipe blanks using centrifugal casting technology with rotation in horizontal axis. Value t_T determines liquid alloy portion, which solidification accompanied by shrinkage porosity or crumbles appearance in casting. In foundry shops this parameter is used, in particular, to predict directionally crystallized castings quality, to determine cast iron rolling rolls electric arc heating time, etc.

For many critical purposes cast parts one of indicators is their tightness level, which depends on size and nature of shrinkage (gas-shrinkage) pores distribution in casting walls. At the same time, other conditions being equal, shrinkage (gas-shrinkage) porosity value and its distribution nature in casting sections depend on both value of Δt_{LS} and value of t_T, as well as solid phase relative fraction in crystallization temperatures range (A. Bochvar, 1952, S. Rep'yakh, 1984, 2006).

Under any mechanism, shrinkage (gas-shrinkage) porosity occurrence is caused by filtration mass transferring cessation by casting (ingot, slab, bloom) melt from supply source to its crystallization front in the two-phase region. Therefore, definition liquidus (t_L) and solidus (t_S) temperatures values, crystallization temperature interval Δt_{LS} value, solid phase kinetics and appearance nature, its relative volume fraction in alloy two-phase region, establishing the synergistic and selective influence of its chemical elements on temperatures t_L, t_S and Δt_{LS} value is an important characteristic and an actual research task for any casting alloy and for cast products manufacturing by any methods from it conditions.

Literature review. Phase diagrams for significant number of two-component alloys presence allows to determine fairly accurately and quickly their temperatures t_L, t_S and value of Δt_{LS} in mass and atomic changes in both alloy components content entire range [5, 6]. There are much smaller number of ternary alloys phase diagrams, which are result of ternary alloy phase equilibria 3D triangular diagram constructing or its concentration triangle projection onto the plane [7]. Alloys with four or more components phase diagrams are problematic issue, which is explained by constructing and presenting them in three-dimensional space impossibility. Therefore, as a rule, studies results graphic representation of any alloying component influence on multicomponent alloy phase transformation temperatures is its individual phase diagrams with figurative points. To construct them, main and other alloying components fixed amount in alloy is represented as a single pseudo-element. That is, in essence, such phase diagrams are phase transformations reflection in two-component system of pseudo-element (including alloy's basic component) and alloying element under study [8].

It should be noted that all existing phase diagrams are result of certain chemical composition alloys thermography generalizing during their melts cooling in mold at certain rate or by conducting alloys differential thermal analysis during their melts cooling at given constant rate [9, 10]. At the same time, when liquidus and solidus temperatures determining, it should take into account in any technical purity alloy uncontrolled impurities presence, which usually leads to changes in its characteristic temperatures values due to change in nucleation mechanism from homogeneous to heterogeneous. Therefore, one of research tasks into crystallization temperature range has always been mathematical models development for exact or with an acceptable absolute error values numerical definition for alloys' liquidus and solidus temperatures by calculation.

Solving this challenge, Shmrga L. (1985) proposes to calculate liquidus and solidus temperatures for carbon and alloy steels using formula

$$\Delta T = (1 - k_0) \cdot N_L \cdot R \cdot (T_M)^2/\mathrm{L}, \qquad (1)$$

where k_0 is individual coefficient for each chemical element of steel for liquidus and solidus temperatures, which is determined by corresponding binary phase diagram; N_L is impurity element in iron mole fraction; R is gas constant; T_M is pure iron melting temperature, K; L is iron fusion molar latent heat.

Zadumkin S. (1960) suggests calculating steels liquidus temperature using formula

$$T_L = T_M - \left\{\sum (a_0 + a_1[i] + a_2[i])\right\}, \qquad (2)$$

where T_M is pure iron melting temperature, °C; a_0 is pure iron melting point reduction factor (implemented when accepting temperature value $T_M > 1{,}539$ °C); a_1, a_2 are empirical coefficients of first and second order significance for corresponding element "i", which is in given steel grade; [i] is content of "i"th chemical element in this steel grade, %.

Liquidus temperature experimental and calculated by formula (2) values comparison, carried out by A. Smirnov and colleagues (1996), showed that for carbon steels the difference between calculated and experimental values reaches 57 °C, and for alloyed steels 80 °C.

Significant error in a case of using formulas (1) and (2) is also noted in S. Kabyshov, et al. (2015) work, in connection with which they propose to use following formula for solidus temperature calculation

$$T_S = T_L - \sum (a_0 + a_1[i] \cdot (1 + k_{l,i})); \qquad (3)$$

$$k_{li} = 1 - K_i,$$

where $k_{l,i}$ is coefficient of "i"th chemical element distribution between solid and liquid phases during equilib-

rium crystallization; K_i is liquation coefficient of "i"th chemical element in binary alloy.

As in formulas (1 and 2), formula (3) contains empirical coefficients, which, due to the lack of uniform methodology, have been determined by researchers Andrews K. (1981), Kawakami K. (1982), Kagava A. (1986), Schrewe H. (1987) and others using their own original methods. As a result, the calculation according to formulas (1–3) does not allow obtaining calculated temperatures acceptable values. In this regard, the above formulas have purely theoretical significance and require clarification and certain refinements.

To determine synergistic and selective alloy donations components effect on values of t_L and t_S, above experimental methods usually use alloys with particular alloying element variable content. Based on obtained experimental data results graphical or mathematical processing, graphical dependences are constructed, respectively, or mathematical models are used in linear or nonlinear polynomials form, according to which their authors propose to calculate t_L, t_S temperatures. That is, in some cases calculation formulas for t_L and t_S are first order linear polynomials with respect to alloy components content, in others they are second order polynomials (A. Smirnov and colleagues, 1996, 2000, 2005), for example, of the form

$$t_L = t_{L,BASE} - \sum 100[p_{L,i} \cdot (x_{L,i})^2 + q_{L,i} \cdot x_{L,i}]; \quad (4)$$

$$t_S = t_{S,BASE} - \sum 100 \cdot [p_{S,i} \cdot (x_{S,i})^2 + q_{S,i} \cdot x_{S,i}], \quad (5)$$

where $p_{L,i}$, $q_{L,i}$ and $p_{S,i}$, $q_{S,i}$ are regression coefficients in binary system; $x_{L,i}$, $x_{S,i}$ is element mole fraction in an alloy; $t_{L,BASE}$, $t_{S,BASE}$ are temperatures liquidus and solidus of alloy's base

Calculation using formulas (4 and 5) accuracy comparison, performed by K. Zubarev and colleagues (2016), shows that liquidus temperature difference between real and theoretical values for 24 multicomponent (complex alloying) nickel-based alloys is in the range from –24 to +32 °C. At the same time, K. Zubarev, et al. (2016) note that binary parameters p_L and q_L for complex nickel-based alloys extended array using allows to put into service formula (4) to calculate their liquidus temperature with an accuracy of ±19.8 °C, which, from K. Zubarev's point of view, is sufficient reason to recommend formula (4) for practical application.

This work authors opinion that an error of ±19.8 °C is unacceptable for conducting synergistic and selective analysis of any alloy's doping components influence on its reference points, and therefore these formulas require some developing. In addition, it is not clear what formulas' (4 and 5) developers meant by introducing the values $t_{L,BASE}$, $t_{S,\ BASE}$ into their composition if any alloy basis is pure metal that does not have in its characteristics melting point into liquidus and solidus division.

Formulas example in linear polynomial model form are the formulas of V. Denisov and A. Denisov (1983), according to which the temperatures t_L, t_S and Δt_{LS} value for low and medium alloyed steel grades with content: Co ≤ 15 %; W ≤ 12 %; Al ≤ 10 %; Mn ≤ 9 %; Cu, Mo ≤ 7 %; Si, Cr, V, Zr ≤ 5 %; Ni, Ti ≤ 3 %; B ≤ 0.1 %; P ≤ 0.7 %; S ≤ 0.08 %; N, O ≤ 0.03 %, authors propose to calculate, based on alloying elements mass content (%) in them, °C

$$t_L = 1{,}539 - 78 \cdot C - 12 \cdot Si - 5 \cdot (Mn + Cu) - 1.5 \cdot (Cr + W) - 4 \cdot Ni - 2 \cdot (Mo + V + Al + Co) - 10 \cdot Ti - 150 \cdot B - 6 \cdot Zr - 30 \cdot P - 25 \cdot S - 80 \cdot O - 90 \cdot N - 1{,}300 \cdot H; \quad (6)$$

$$t_S = t_L - [13 + 140 \cdot C + 4.5 \cdot (Si + Ni) + 2.5 \cdot Mn + Cr + 3 \cdot (Cu + Mo + V + W + l) + Co + 5 \cdot Ti]. \quad (7)$$

Temperature (t_S) is calculated using formula

$$t_S = t_L - \Delta t_{LS}; \quad (8)$$

$$\Delta t_{LS} = \Delta t_C + \Delta t_{El}, \quad (9)$$

where Δt_C, Δt_{El} is steel crystallization temperature range depending on carbon and other chemical elements content, respectively, °C.

$$\Delta t_C = 13 + 140 \cdot C; \quad (10)$$

$$\Delta t_{El} = 4.5 \cdot (Si + Ni) + 2.5 \cdot Mn + Cr + 3 \cdot (Cu + Mo + V + W + Al) + Co + 5 \cdot Ti. \quad (11)$$

From equations (6–11) analysis it follows that in low- and medium-alloyed steel grades temperatures t_L and t_S dependence on chemical elements mass content within their specified limits changes is exclusively linear, and their synergistic effect corresponds to additivity rule. Based on the fact that practically every chemical element presented in formulas (6–11) with iron in binary alloys has nonlinear dependences on both temperatures t_L and t_S, it is easy to assume that with alloying components content and number in steel increasing, error between real and calculated data t_L and t_S will increase. Therefore, values' reliability that can be calculated using formulas (6–11) for multicomponent steels is questionable. As noted above, other things being equal, melt solidification nature, macrostructure, location nature of the shrinkage porosity volume along castings walls cross-section, which, in turn, determine their tightness level, also depend on Δt_{LS} value. That is, in casting production in foundries conditions using generally accepted technologies, with Δt_{LS} value increasing, melt solidification in casting mold nature changes from sequential to mixed and volumetric. At the same time, with Δt_{LS} value increasing, alloys mechanical properties level increases, probability of crumbling and shrinkage cavities in castings decreases, but cast parts tightness decreases, casting peel thickness on castings surfaces decreases and shrinkage (gas-shrinkage) porosity zone size and width increases.

According to A. Veynik (1964), in casting alloy solidification sequential nature occurs under condition

$$\frac{\Delta t_{LS}}{\delta \cdot (t_L - t_{sc})} \ll 1, \quad (12)$$

where t_{SC} is casting surface temperature, °C; δ is casting wall thickness, m.

Accordingly, casting melt solidification has volumetric nature if solidification satisfies following condition

$$\frac{\Delta t_{LS}}{\delta \cdot (t_L - t_{sc})} \gg 1. \quad (13)$$

That is, when condition (12), which is realized at high intensity of heat removal from casting into the

mold, is fulfilled, solid phase in the melt sequent grows realizes. If condition (9) is fulfilled before melt solidification in casting wall is complete, then solidified alloy acquires trans-crystalline structure.

One of alloys' two-phase region significant indicators that affects shrinkage defects (porosity, crumbles and shells) value and thickness of casting peel on castings is solid phase in it relative volume fraction (φ_{SP}). φ_{SP} value depends exclusively on alloys' chemical composition and, in particular, according to S. I. Repyakh (2006), are: 0.55 for steel 04Х13Н5М5К9Л; 0.87 for steel 10Х16Н3Л; 0.84 for aluminum alloy АЛ8; 0.69 for bronze БрО10Ц2. With φ_{SP} value decreasing, porous zone width in castings walls' cross-sections decreases; shrinkage defects total value decreases and casting peel thickness on castings increases. This significantly increases cast parts tightness and reliability.

Today, there are various hypotheses regarding shrinkage (gas-shrinkage) porosity causes and mechanisms. Only thing that unites all these hypotheses is that any shrinkage discontinuities in castings arise in melt filtration flow continuity disruption event from riser or feeder to the melt crystallization front. But, in any case, filtration processes beginning and completion of castings solidification in two-phase liquid-solid region occurs at solid phase certain relative volumetric amount in it. In particular, according to A. Veinyk (1960), V. Bondarev (1963) and A. Naryvsky (1976), solid phase relative volume fraction in aluminum-silicon alloys crystallization temperature range at the moment of shrinkage porosity appearance is 80–95 %. At the same time, A. Veinyk (1960) believes that filtration mass transfer initiation begins at solid phase volume content φ_{SSP} = = 20–40 % and finalizes at φ_{FSP} = 80–90 %. That is, with 80–90 % solid phase content in crystallization temperature range of these alloys, shrinkage porosity begins to appear between neighboring dendrites branches from melt residues disconnected from power source.

φ_{SSP} and φ_{FSP} values change as a result of external influences on the melt in casting mold and depend on melt purity and its chemical composition. In particular, according to research by O. Magnytsky, B. Gulyaev (1960), E. Siegfrid and H. Leonhard (1973) results, with silicon in Al-Si alloy mass content increasing from 1 to 10 %, primary solid phase amount, which creates single dendritic skeleton, changes in volume, respectively, from 90 to 60 %. It follows from this, depending on silicon content in Al-Si alloy, melt filtration mass transfer begins with 90–60 % solid phase excretion in crystallization temperature range. Accordingly, remaining solid phase 10–40 % is in unconnected crystals form in layer whose limits are between liquidus temperature and melt residue pouring temperature – t_P.

According to Fe-C alloys shrinkage feeding process modeling results, proposed by A. Ryzhikov and G. Timofeev (1972, 1973), it was established that filtration mass transfer in Fe-C alloys two-phase region begins at solid phase volume content in it of 50–60 %. At the same time, liquid phase movement speed in inter-dendritic space during filtration, for example in tin bronze, according to A. Narivsky and colleagues (1976), does not exceed 0.3 mm/s and in most cases is ~0.1 mm/s.

As for bronze БрА7К2О1,5Мц0,3, there are currently no formulas for its temperatures t_L, t_S calculating and interval Δt_{LS} value, also φ_{SP} and kinetics of solid phase excretion in crystallization temperature range, which are any alloy fundamental parameters, have not been established. There is also no data on its conditionally true fluidity, selective and synergistic effect of its main alloying chemical elements on t_L temperature and temperature interval Δt_{LS}. Therefore, work devoted to determining bronze БрА7К2О1,5Мц0,3 components influence on above mentioned parameters is relevant.

Purpose. For Cu-Al-Si-Sn-Mn system bronzes, to establish quantitative values of its crystallization interval indicators (liquidus, solidus temperatures, interval size and solid phase formation in it relative proportion) and to determine synergistic and selective alloying components of bronze БрА7К2О1,5Мц0,3 influence on these indicators and relative fluidity changing.

Methodology. Research has been conducted on bronzes that were melted in air in graphite crucible of induction furnace under charcoal layer. Following grades of technical purity have been used as charge materials: cathode copper М2, aluminum Al99.7, silicon Кр1, tin О1, and silicomanganese МнС17. Alloys chemical composition has been determined on EXPERT 4L precision analyzer.

Bronze БрА7К2О1,5Мц0,3 with chemical elements given in Table 1 content has been used in the present research.

Studied bronzes temperatures t_L, t_S and solid phase exudation kinetics in Δt_{LS} interval have been determined on synchronous thermal analyzer STA 449 C "Jupiter" of NETZSCH Co. (Germany) by studied samples heating to 1,210 °C and their subsequent cooling at a rate of 20 °C/min in argon environment. Temperatures t_L, t_S have been also determined based on bronze samples ∅19 × 50 mm thermography results which have been cast in air into sand-sodium-silicate casting mold.

Melt and thermography temperature measurement have been performed using chromel-alumel thermocouple with unprotected hot junction (electrodes hot junction diameter – 0.3 mm) completed with electronic potentiometer, which has measurement results electronic protocols forming and archiving option. Water and air temperature has been measured with ТТЖ type alcohol thermometer with accuracy of ± 1 °C.

To determine kinetics and solid phase portion in temperature interval Δt_{LS}, graphical dependences ($\varphi_{SP} = f$) have been used. These dependences have been constructed based on differential thermal analysis results.

Table 1

Alloying elements and impurities content in bronze БрА7К2О1.5Мц0.3

Chemical element	Al	Si	Mn	Sn	nn (impurities)
Content, % (mass)	6.0–7.5	1.0–2.5	0.21–0.45	1.0–2.2	≤0.45

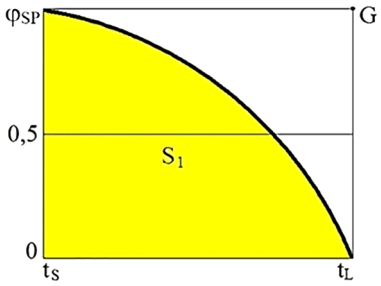

Fig. 1. Scheme for solid phase amount in bronze crystallization temperatures interval calculating

Value φ_{SP} calculation has been carried out according to the scheme in Fig. 1 using the formula

$$\varphi_{SP} = S_1 / S_2, \quad (14)$$

where S_1 is surface area under the curve in Fig. 1 (shaded in yellow); S_2 is graphic image in Fig. 1 surface area between points $t_S - \varphi_{SP} - G - t_L$.

Areas S_1 and S_2 determination has been carried out using digital image analysis method.

Solid phase volume content on temperature graphical dependences in Δt_{LS} interval for alloys copper with 7 % Al, copper with 2 % Sn and copper with 2 % Si have been plotted based on calculations according to lever rule results [11] using binary phase diagrams of Cu-Al [12, 13], Cu-Sn [12, 13] and Cu-Si [12] systems.

To determine bronze БрА7К2О1,5Мц0,3 alloying components synergistic and selective effect on temperature t_L and temperature interval Δt_{LS}, criterion K_R has been used. For given bronze this criterion is its alloying elements and undesirable impurities mass content ratio, which is presented as [14]

$$K_R = (1 - 0.01 \cdot nn) \cdot \frac{\text{Al-Si-Mn}}{(1+\text{Sn})^2}, \quad (15)$$

where *nn* is undesirable impurities mass content, %; Al, Si, Mn, Sn are, respectively, aluminum, silicon, manganese, tin mass content, %, and additionally polynomial models of the functions $t_L = f(K_R)$ and $\Delta t_{LS} = f(K_R)$, which were obtained based on experimental data computer processing results using Excel program.

Alloying elements in bronze БрА7К2О1,5Мц0,3 content selective influence on the change in its chemical composition analysis at K_R criterion constant value has been carried out based on isolines constructing results of K_R accepted limits change in simplex triangles, plotted according to incomplete cube plan-matrix in H. Scheffer's passive experiments ternary system. "Key" (red arrows) is presented in Fig. 2.

According to H. Scheffer's plan, incomplete cube mathematical model in ternary system is

$$Y = \beta_1 \cdot x_1 + \beta_2 \cdot x_2 + \beta_3 \cdot x_3 + \beta_{12} \cdot x_1 \cdot x_2 + \beta_{13} \cdot x_1 \cdot x_3 + \\ + \beta_{23} \cdot x_2 \cdot x_3 + \beta_{123} \cdot x_1 \cdot x_2 \cdot x_3, \quad (16)$$

where Y is material's property; β is regression coefficient; x is chemical element mass content in alloy, %.

Regression coefficients in formula (20) calculation have been carried out using the following equations

$$\beta_1 = \xi_1; \quad \beta_{ij} = 4 \cdot \xi_{ij} \; 2 \cdot \xi_i - 2 \cdot \xi_j; \\ \beta_{123} = 27 \cdot x_{123} - 12 \cdot (x_{12} + x_{13} + x_{23}) + \\ + 3 \cdot (x_1 + x_2 + x_3), \quad (17)$$

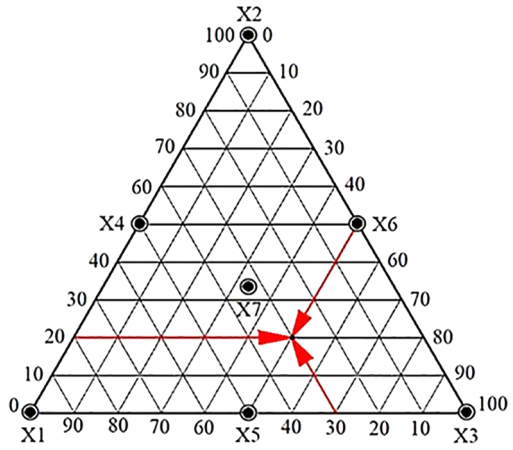

Fig. 2. Simplex triangle of incomplete third degree polynomial with "key" (red arrows)

where ξ_i, ξ_j, ξ_{123} are investigation results in simplex lattices points (Fig. 1).

As representative from aluminum bronzes group, for bronze БрА7К3О1,5Мц0,3 relative conditionally true fluidity assessing, alloy БрА9Ж3Л has been chosen as one most often used in foundries for cast shaped bronze parts manufacturing. Bronzes conditionally true fluidity has been estimated by spiral test at their melts overheating value of 150–160 °C.

To produce spiral probe, casting molds have been used from sand-sodium-silicate mixture containing 6 % sodium-silicate solute and 94 % by weight quartz sand grade $1K_2O_202$. Before use, manufactured half-molds for spiral probe have been dehydrated in dryer at 120–140 °C for 48–50 hours, after which they have been cooled in air to temperature of 22–25 °C.

To calculate БрА7К3О1,5Мц0,3 bronze relative conditionally true fluidity, 2–3 its tests results average values for each K_R value have been divided by 2 studies similar result for БрА9Ж3Л bronze.

Results. Chemical composition, K_R criterion value, liquidus and solidus temperatures and Cu-Al-Si-Sn-Mn system bronzes with $K_R = 0.35–0.84$ [14] crystallization temperature interval determining results are given in Table 2.

According to Table 2 data, dependences between K_R criterion, liquidus temperature (t_L) and crystallization temperature interval (Δt_{LS}) for bronzes with $K_R = 0.35–0.84$ have been constructed and presented in Fig. 3.

From dependencies in Fig. 3 course analysis it follows that in Cu–Al–Si–Mn–Sn system bronzes, to which brand БрА7К2О1,5Мц0,3 bronze belongs, with K_R increasing from 0.35 to 0.84, crystallization temperature interval increases from 32 to 49 °C, and liquidus temperature decreases from 1,008 to 997 °C at $K_R \approx 0.47$, after which it monotonically increases to 1,027 °C.

Thus, for bronze БрА7К2О1,5Мц0,3, in which $K_R = 0.35–0.84$, liquidus temperature ($R^2 = 0.97$) value as well as crystallization temperature interval ($R^2 = 0.97$) value have been calculated by the formulas

$$t_L = 995.4 + 512 \cdot K_R - 2{,}475.5 \cdot (K_R)^2 + \\ + 3{,}834 \cdot (K_R)^3 - 1{,}855 \cdot (K_R)^4; \quad (18)$$

$$\Delta t_{LS} = 105.4 - 491 \cdot K_R + 1{,}101 \cdot (K_R)^2 - \\ - 920 \cdot (K_R)^3 + 250 \cdot (K_R)^4. \quad (19)$$

Table 2

Chemical composition, K_R criterion value, liquidus and solidus temperatures, Cu-Al-Si-Sn-Mn system bronzes with $K_R = 0.35–0.84$ crystallization temperature interval

No.	Chemical elements content, % (mass)						K_R	t_L, °C	t_S, °C	Δt_{LS}, °C
	Cu	Al	Si	Mn	Sn	nn				
1	91.4	5.84	1.12	0.01	1.37	0.26	0.84	1,027	978	49
2	88.6	6.7	1.79	1.07	1.23	0.61	0.77	1,021	973	48
3	87.63	7.5	2.5	0.5	1.55	0.32	0.69	1,010	963	47
4	88.83	6.8	1.94	0.27	1.66	0.38	0.65	1,001	960	41
5	88.03	6.99	2.41	0.41	1.81	0.39	0.52	998	960	38
6	87.8	7.12	1.24	0.96	2.26	0.62	0.46	997	963	34
7	89.07	7.31	2.49	0.48	2.25	0.19	0.41	999	967	32
8	88.92	6.02	2.09	0.32	2.2	0.45	0.35	1,009	976	33

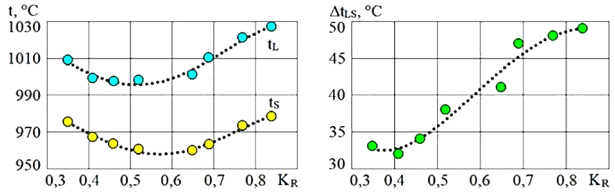

a *b*

Fig. 3. Liquidus and solidus temperatures (a) and Cu-Al-Si-Sn-Mn system bronze crystallization temperature interval (b) dependences on criterion K_R value

Temperatures t_S have been calculated using the formula

$$t_S = t_L - \Delta t_{LS}, \quad (20)$$

or according to the formula ($R^2 = 0.99$)

$$t_S = 885.2 + 1,027 \cdot K_R - 3,613 \cdot (K_R)^2 + \\ + 4,765 \cdot (K_R)^3 - 2,098 \cdot (K_R)^4. \quad (21)$$

Relative errors between calculated using formulas (18, 19) data and experimental results have been estimated according to the formulas, %

$$\Delta_L = 100 \cdot (t_{Le} - t_{Lc})/t_{Le}; \quad (22)$$

$$\Delta S = 100 \cdot (t_{Se} - t_{Sc})/t_{Se}; \quad (23)$$

$$\Delta_{LS} = 100 \cdot (\Delta t_{LSe} - \Delta t_{LSc})/t_{LSe}, \quad (24)$$

where t_{Le}, t_{Se}, Δt_{LSe} are liquidus, solidus and bronze crystallization temperature range experimental values, respectively, °C; t_{Lc}, t_{Sc}, Δt_{LSc} are values calculated by formulas (18, 21, 19), respectively, °C.

K_R criterion, experimental and calculated values of liquidus temperature and bronzes crystallization temperature interval, calculated according to formulas (16) and (17), and their errors, which have been calculated according to formulas (22–24), are given in Table 3.

From data in Table 3 analysis, it follows that errors between calculated and experimental data does not exceed 6 %, which gives reason to recommend formulas (18, 19 and 21) using for bronze БрА7К2О1,5Мц0,3 in processes of modeling and predicting its properties, in particular, liquidus and solidus temperatures and crystallization temperature range.

From dependences in Fig. 3 analysis it follows that for bronze БрА7К2О1,5Мц0,3 with K_R criterion value from 0.42 to 0.52 liquidus temperature monotonically decreases from 1,009 to 998 °C, but from $K_R = 0.52$ to 0.84 it increases to 1,028 °C. Solidus temperature increases in almost the same way. At the same time, with K_R criterion value increasing from 0.42 to 0.84, bronze crystallization temperature interval "expands" from 32 to 49 °C.

From practical point of view, this means that bronze БрА7К2О1,5Мц0,3 is alloy with "narrow" crystallization temperature range. That is, this bronze, under certain

Table 3

Criterion K_R, experimental and calculated according to formulas (18, 19 and 21) values of liquidus, solidus temperatures, bronzes crystallization temperature interval and their errors (D), which have been calculated according to formulas (22–24)

K_R	t_L, °C		Δ_L, %	t_S, °C		Δ_S, %	Δt_{LS}, °C		Δ_{LS}, %
	Exp.	Calc.		Exp.	Calc.		Exp.	Calc.	
0.84	1,027	1,027.4	–0.04	978	978.2	0.01	49	49.0	–0.01
0.77	1,021	1,020.0	0.10	973	971.7	0.13	48	48.0	0.03
0.69	1,010	1,009.0	0.12	963	963.5	–0.03	47	45.2	3.75
0.65	1,001	1,004.0	–0.31	960	960.3	–0.05	41	43.4	–5.84
0.52	998	995.7	0.24	960	958.9	0.13	38	36.7	3.39
0.46	997	997.2	–0.02	963	963.0	0.00	34	34.2	–0.46
0.41	999	1,001.0	–0.20	967	968.0	–0.11	32	32.8	–2.58
0.35	1,009	1,007.9	0.07	975	974.9	0.05	33	32.7	0.82

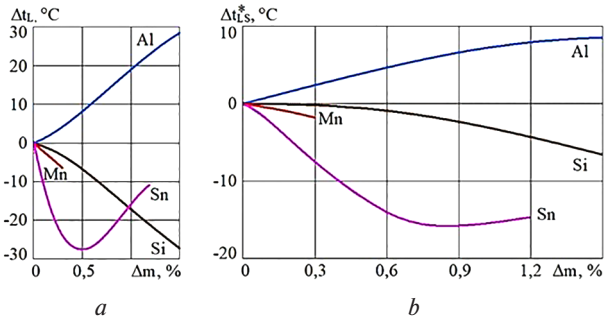

a *b*

Fig. 4. Changes in liquidus temperature (a) and bronze БрА7К2О1,5Мц0,3 crystallization temperature interval (b) dependences on changes in alloying elements in its composition mass content

conditions, is prone to columnar macrostructure appearance, and its alloying components content within limits above has negligible effect on changes in t_L, t_S and Δt_{LS}.

Equations (8 and 18) have been used to calculate, construct dependencies and analyze bronze БрА7К2О1,5Мц0,3 alloying components selective influence on changes in its crystallization temperature interval.

The dependences of changes in bronze БрА7К2О1,5Мц0,3 liquidus temperature (Δt_L) and crystallization temperature interval (Δt^*_{LS}) from changes in alloying elements (Δm) mass content in its composition are presented in Fig. 4.

From dependences in Fig. 4 analysis, it follows that Al increases, Mn and Si decrease both liquidus temperature and БрА7К2О1,5Мц0,3 crystallization temperature interval. Sn content increasing from 1.0 to 1.5 % reduces t_L value and subsequently (up to 2.2 %) increases it. Meanwhile, Sn content increasing from 1.0 to 1.8 % reduces Δt_{LS} and with further increasing in content to 2.2 %, it slightly increases it. This chemical elements influence nature (Fig. 3) on t_L and Δt_{LS} values could not be predicted based on binary diagrams phase composition analysis results, in particular, Cu-Si, Cu-Sn and Cu-Mn systems, in which binary bronzes Δt_{LS} value increases with silicon, manganese and tin mass fraction increasing. This discrepancy has been explained by the fact that, probably, during bronze melt crystallization, intermetallics appear in its structure as diffusion reaction result at interface between solid and liquid phases, for example, by chemical reaction undergoing, whose rate is not related to reacting components mutual solubility, but to components in both phases concentration ratio changing at crystallization front and/or by components diffusion from liquid to solid phase, which leads to solid solution crystal lattice reorganization into intermetallic lattice upon solubility limit reaching (V. Bugakov, 1949; N. Lashko, 1977; S. Bokshtein, 1978). Therefore, regardless of intermetallic formation mechanism, reaction diffusion leads to melt depletion in chemical elements which are intermetallics part, and, accordingly, to enrichment in components that are indifferent to reaction and, as a result, to Δt_{LS} value changing.

Data obtained indicate that in alloying elements mass content in БрА7К2О1,5Мц0,3 bronze composition slight changing within accepted limits leads to rather unpredictable change in its crystallization temperature range. Furthermore, this suggests that widely applied binary phase equilibria diagrams using for analyzing and predicting phase transition temperatures and temperature ranges for multicomponent alloys is not perfectly comprehensive.

Based on above, to achieve desired compromise between mechanical and casting properties levels, bronze БрА7К2О1,5Мц0,3 must meet required K_R criterion value in the range from 0.35 to 0.84.

This requirement is due to the fact that this bronze multicomponent nature, with its alloying components certain combinations within grade composition range, may not meet permissible changes in K_R criterion specified limits. This will naturally lead to the bronze increased brittleness or low strength.

This is confirmed by virtual experiment results with bronze БрА7К2О1,5Мц0,03, in which chemical composition only tin, silicon or aluminum content has been alternately changed.

Alloying elements in bronze БрА7К2О1,5Мц0,3 content selective influence on its chemical composition changing, with criterion K_R constant value, analysis has been carried out using an imaginary factorial experiment planning. To conduct such an experiment, simplex experimental planning has been applied using H. Scheffer method, in which response function was criterion K_R = = 0.65–0.7 value. Elements in bronzes mass content and their K_R coefficient values are given in Table 4.

Regions with K_R = 0.65–0.7 values position changes (“drift”) depending on alloying components content changes in bronze БрА7К2О1,5Мц0,3 composition has been studied on simplex triangles response surfaces, which have been calculated according to the data in tables 4–6 and are presented in Fig. 5.

Table 4

Elements and impurities mass content in bronzes, their coefficient K_R values at fixed Sn content

n/o	Elements ad impurities mass content, %				K_R with Sn content in bronzes, %		
	Al	Si	Mn	nn	1.4	1.6	1.8
X1	7.5	1.5	0.3	0.4	0.986	0.840	0.724
X2	7	1.8	0.3	0.4	0.847	0.722	0.623
X3	6	22	0.3	04	0.605	0.516	0.445
X4	7.25	1.65	0.3	0.4	0.916	0.781	0.673
X5	6,75	1.85	0.3	0.4	0.795	0.678	0.584
X6	6.5	2	0.3	0.4	0.726	0.619	0.534
X7	6.83	1.83	0.3	0.4	0.813	0.692	0.597

Table 5

Elements and impurities mass content in bronzes, their coefficient K_R values at fixed Si content

n/o	Elements and impurities mass content, %				K_R with Si content in bronzes, %		
	Al	Sn	Mn	nn	1.4	1.6	1.8
X1	7.5	1.5	0.3	0.4	0.924	0.892	0.861
X2	7	1.8	0.3	0.4	0.673	0.648	0.623
X3	6	2.2	0.3	0.4	0.418	0.399	0.379
X4	7.25	1.65	0.3	0.4	0.787	0.759	0.730
X5	6.75	1.85	0.3	0.4	0.619	0.595	0.570
X6	6.5	2	0.3	0.4	0.531	0.509	0.487
X7	6.83	1.83	0.3	0.4	0.637	0.612	0.587

Table 6

Elements and impurities mass content in bronzes, their coefficient K_R values at fixed Al content

n/o	Elements and impurities mass content, %				K_R with Al content in bronzes, %		
	Sn	Si	Mn	nn	7.0	7.2	7.4
X1	2.2	1.5	0.3	0.4	0.506	0.525	0.545
X2	1.8	1.8	0.3	0.4	0.623	0.648	0.673
X3	1.5	2.2	0.3	0.4	0.717	0.749	0.781
X4	2	1.65	0.3	0.4	0.559	0.581	0.603
X5	1.85	1.85	0.3	0.4	0.595	0.619	0.644
X6	1.65	2	0.3	0.4	0.667	0.695	0.723
X7	1.83	1.83	0.3	0.4	0.604	0.629	0.653

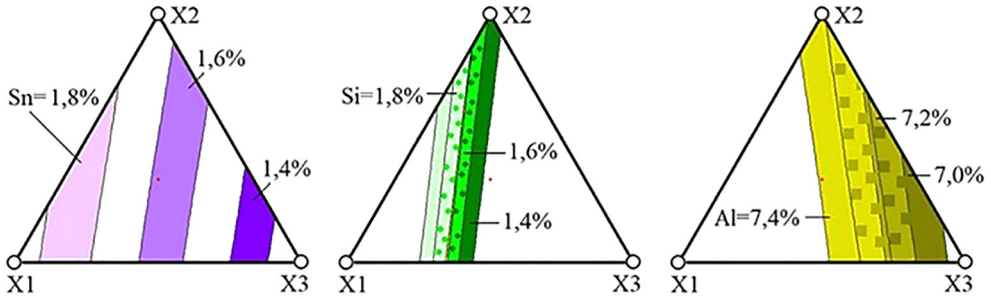

a *b* *c*

Fig. 5. Areas corresponding to K_R = 0.65–0.70 values interval when tin (a), silicon (b), aluminum (c) content changing in bronze

From dependencies in Fig. 5 character analysis, it follows that obtaining bronze БрА7К2О1,5Мц0,3 with mechanical and casting properties desired level (with a given criterion K_R value) requires not only its alloying elements content in bronze within its grade ensuring, but also a certain K_R value.

Criterion K_R value for bronze БрА7К2О1,5Мц0,3 can be adjusted by adding Si, Mn, Sn, or Al certain amount to its melt during melting. At the same time, corresponding charge mixture mass must take into account its alloying element (elements) combustion. In such cases, material selected limits for adjustment can be calculated using transformed formula (15). In particular, when using tin to adjust K_R value, the of its maximum and minimum amount in bronze (excluding melting combustion loss) calculation, assuming desired K_R change interval within the range from its minimum ($K_R^{\min}$) to its maximum ($K_R^{\max}$) value and undesirable impurities content in bronze equal to zero, can be carried out according to formula, where chemical elements content is indicated in % by mass, % (wt.)

$$\begin{cases} \mathrm{Sn}_{\max} = \sqrt{\dfrac{\mathrm{Al\text{-}Si\text{-}Mn}}{K_R^{\min}}} - 1 \\ \mathrm{Sn}_{\min} = \sqrt{\dfrac{\mathrm{Al\text{-}Si\text{-}Mn}}{K_R^{\max}}} - 1 \end{cases}; \qquad (25)$$

- using manganese for adjustment, % (wt.)

$$\begin{cases} \mathrm{Mn}_{\max} = \mathrm{Al\text{-}Si\text{-}}K_R^{\min} \cdot (1+\mathrm{Sn})^2 \\ \mathrm{Mn}_{\min} = \mathrm{Al\text{-}Si\text{-}}K_R^{\max} \cdot (1+\mathrm{Sn})^2 \end{cases}; \qquad (26)$$

- using silicon for adjustment, % (wt.)

$$\begin{cases} \text{Si}_{max} = \text{Al-Mn-}K_R^{min} \cdot (1+\text{Sn})^2; \\ \text{Si}_{min} = \text{Al-Mn-}K_R^{max} \cdot (1+\text{Sn})^2; \end{cases} \quad (27)$$

- using aluminum for adjustment, % (wt.)

$$\begin{cases} \text{Al}_{max} = \text{Si} + \text{Mn} + K_R^{max} \cdot (1+\text{Sn})^2 \\ \text{Al}_{min} = \text{Si} + \text{Mn} + K_R^{min} \cdot (1+\text{Sn})^2 \end{cases}. \quad (28)$$

For formulas (25–28) practical implementation, when calculating charging materials, it is also necessary to take into account iron, nickel and cobalt total content, which should not exceed 0.17 % by weight in charge materials. This will ensure that bronze has no magnetic properties and that alloying elements have been burned at acceptable level during bronze melting.

Solid phase relative volume fraction in bronzes' crystallization temperature interval. Solid phase (φ_{SP}) relative volume fraction changes dependences in crystallization temperature interval for Cu-Al-Si-Sn-Mn system bronzes, which are obtained from differential thermal analysis data results processing, are presented in Fig. 6. The same figure shows similar dependences calculated by the lever rule (segment rule) [11] for copper alloys with 7 % Al, copper with 2 % Sn and copper with 2 % Si. For these curves plotting, double phase diagrams of Cu-Al [12, 13], Cu-Sn [12, 13] and Cu-Si [12] systems have been used.

From dependences in Fig. 6 character analysis, it follows that solid phase distribution nature in Cu-Al-Si-Sn-Mn system studied bronzes crystallization temperature interval within K_R changes range from 0.35 to 2.07 practically does not depend on their K_R index value. At the same time, solid phase (φ_{SP}) relative volume fraction for these bronzes in crystallization temperature interval is 61–63 %. It is significant that φ_{SP} value for bronze with 7 % Al is 53 %, for bronze with 2 % Sn – 77 %, and for copper with 2 % Si – 56 %. That is, this indirectly indicates that aluminum and silicon presence in studied bronze composition reduces φ_{SP} value, and Sn increases it.

Fluidity. Bronzes БрА9Ж3Л and БрА7К3О1,5Мц0,3 fluidity has been evaluated using spiral-shaped probe, for which manufacturing mold made of sand-sodium-silicate mixture has been used. Molds have been poured at temperature of 1,190–1,200 °C for БрА9Ж3Л bronze melts and 1,160–1,170 °C for БрА7К3О1,5Мц0,3 bronze melts, which in both cases ensured melts overheating at the level of 150–160 °C. That is, under such melt overheating conditions, studied bronzes conditionally true fluidity has been determined.

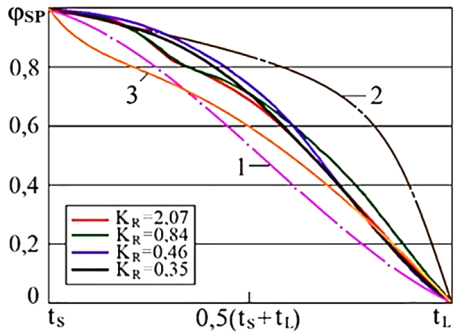

Fig. 6. Solid phase volume fraction (φ_{SP}) dependence in Cu-Al-Si-Sn-Mn system bronzes crystallization temperature range with K_R different values, copper alloy with 7 % Al (1), copper with 2 % Sn (2) and copper with 2 % Si (3)

For БрА9Ж3Л bronze fluidity absolute value according to spiral test was 680–740 mm. БрА7К2О1,5Мц0,3 bronze (relative to БрА9Ж3Л bronze conditional-true fluidity) average relative conditional-true fluidity (Fl) calculating results, using spiral test, are given in Table 7.

From data in Table 3 analysis, it follows that БрА7К3О1,5Мц0,3 and БрА9Ж3Л bronzes conditionally true fluidities are practically the same. That is, bronze БрА7К3О1,5Мц0,3 has sufficiently high level of fluidity, which should positively affect casting surfaces quality. At the same time, any bronze БрА7К3О1,5Мц0,3 conditionally true fluidity value dependence on criterion K_R value has not been established. Dependence $Fl = f(K_R)$ absence for БрА7К3О1,5Мц0,3 bronze could be explained by relatively small change in crystallization temperature interval and liquidus temperature with K_R value changing.

For industrial testing purpose cast bronze БрА7К2О1,5Мц0,3 in foundry, river boat engine propeller shaft hub (casting weight 0.42 kg) and "Bushing" part (casting weight 9.5 kg), which were previously made from БрА9Ж3Л bronze, have been manufactured. River boat engine propeller shaft hub and cast part "Bushing" castings appearance are presented in Fig. 7.

For castings river boat engine propeller shaft hub manufacturing primary charge materials have been used. Melting has been carried out in induction furnace with graphite crucible with metal capacity of 15 kg under charcoal layer. Melt deoxidation has been carried out with manganese in order to obtain 0.2–0.4 % (by weight) residual manganese in alloy. Molten alloy poured from crucible temperature was 1,230–1,250 °C. Casting molds have been made from sand-sodium-silicate mixture using CO_2-process.

According to chemical analysis results and calculation according to formula (2), K_R criterion values were: melt No. 1 – 0.72; No. 2 – 0.49; No. 3 – 0.63; No. 4 – 0.36.

After knocking out and cutting around, castings have been heat treated by quenching them from 750–760 °C into cold water and subsequent aging at 300 ± 10 °C for 1 hour.

According to obtained castings quality assessment results, it was established that castings dimensions correspond to their drawing dimensions. Castings do not have any unacceptable defects that are visually visible (hot cracks, joints, shrinkage crumbling and sinks) and which are inherent in similar БрА9Ж3Л bronze castings. Compared to БрА9Ж3Л bronze, castings manufacturing from БрА7К2О1,5Мц0,3 bronze allowed to reduce machining allowances, increase yield from 0.60 to 0.85 and decrease grooving amount along castings diameter by ~3 times (from 0.3–0.7 mm to 0.1–0.2 mm).

Table 7

Bronze БрА7К3О1,5Мц0,3 vs. bronze БрА9Ж3Л average relative fluidity

K_R	0.84	0.74	0.68	0.59	0.54	0.46
Fl	1.05	0.94	0.99	0.97	1.15	0.97

a *b*

Fig. 7. River boat engine propeller shaft hub (a) and "Bushing" part (b)

Castings made of bronze БрА7К2О1,5Мц0,3 in cast heat-treated state are characterized by good machinability. All machined bushings made of БрА7К2О1,5Мц0,3 bronze have been accepted by "Customer" in terms of quality and have been used in its equipment relevant components without any objurgating during their operation in terms of reliability, durability and performance.

To produce "Bushing" part castings, БрА7К2О1,5Мц0,3 bronze melting has been carried out in induction furnace lined with refractory spinel of SPN 8515-FM brand. Foundry molds have been made from gasified models, which were molded into dry quartz sand for pouring. Bronze melt has been deoxidized with manganese grade Мн-95 to obtain residual manganese in range from 0.1 to 0.5 % by weight. Casting molds have been filled with manual ladle with initial temperature of 450–500 °C. Melt exiting the furnace temperature was 1,200 ± 10 °C.

According to test results, it was found that replacing БрА9Ж3Л bronze with БрА7К2О1,5Мц0,3 (K_R = 0.59) allows to increase the yield from 0.65 to 0.90, and to obtain castings without shrinkage cavities and significant surface defects. Castings made of bronze БрА7К2О1,5Мц0,3 are well processed with blade tool and do not require strengthening heat treatment, since in as-cast state they have hardness of HB = 80–85 units.

According to investigations results and testing in industrial conditions, it follows that structural non-magnetic, corrosion-resistant bronze БрА7К2О1,5Мц0,3 can be recommended for products by casting methods manufacturing, in particular, instead of БрА9Ж3Л brand bronze.

Conclusions. According to investigation results, it was found that for bronze БрА7К2О1,5Мц0,3:

1 – with K_R criterion value increasing from 0.35 to 0.84, temperatures liquidus (999–1,027 °C), solidus (967–978 °C) and crystallization interval (from 32 to 49 °C) increase;

2 – Al in its composition increases, and Mn and Si decrease both liquidus and solidus temperatures and crystallization temperature interval;

3 – Sn content increasing from 1.0 to 1.5 % lowers liquidus temperature, but further increasing content from 1.5 to 2.2 % raises it;

4 – Sn influence on Δt_{LS} value is similar to the influence on liquidus temperature with the difference that Δt_{LS} decreasing occurs with tin content from 1.0 to 1.8 % increasing, and subsequently has practically no effect on Δt_{LS} value;

5 – this bronze conditionally true fluidities and БрА9Ж3Л bronze are practically the same;

6 – according to investigation results and industrial testing, this bronze can be recommended for cast parts manufacturing instead of bronze brand БрА9Ж3Л;

7 – for studied bronze practical implementation, with selected chemical composition within criterion K_R = 0.35–0.84 changes limits, mathematical model of transition from solid phase (φ_{SP}) volume fraction dependences relative values in crystallization temperature range to temperatures absolute values $t(\varphi_{SP})$ has been proposed.

Generally, for Cu-Al-Si-Sn-Mn system's bronzes within K_R changes range from 0.35 to 2.07:

8 – solid phase distribution nature in bronze's crystallization temperature interval's two-phase region practically does not depend on K_R criterion value;

9 – in bronze crystallization's temperature range solid phase relative volume fraction (φ_{SP}) is 60–63 %.

References.

1. Bellón, B., Boukellal, A. K., Isensee, T., Wellborn, O. M., Trumble, K. P., Krane, M. J. M., ..., & LLorca, J. (2021). Multiscale prediction of microstructure length scales in metallic alloy casting. *Acta Materialia*, *207*, 16686. https://doi.org/10.1016/j.actamat.2021.116686

2. Kumar Mohanty, U., & Sarangi, H. (2020). Solidification of Metals and Alloys. *Casting Processes [Working Title]*. IntechOpen. https://doi.org/10.5772/intechopen.94393

3. Liu, Q., Zhang, X., Wang, B., & Wang, B. (2012). Control Technology of Solidification and Cooling in the Process of Continuous Casting of Steel. *Science and Technology of Casting Processes*. InTech. https://doi.org/10.5772/51457

4. Farahany, S., Erfani, M., & Karamoozian, A.O. (2010). Artificial Neural Networks to Predict Liquidus Temperature in Hypoeutectic Al-Si Cast Alloys. *Journal of Applied Sciences, 10*(24), 3243-3249. https://doi.org/10.3923/jas.2010.3243.3249

5. Kőrösy, G., Roósz, A., & Mende, T. (2024). The Concept of the Estimation of Phase Diagrams (An Optimised Set of Simplified Equations to Estimate Equilibrium Liquidus and Solidus Temperatures, Partition Ratios, and Liquidus Slopes for Quick Access to Equilibrium Data in Solidification Software) Part I: Binary Equilibrium Phase Diagrams. *Metals*, *14*(11), 1266. https://doi.org/10.3390/met14111266

6. Okamoto, H. (2019). Supplemental Literature Review of Binary Phase Diagrams: Au-La, Ce-Pt, Co-Pt, Cr-S, Cu-Sb, Fe-Ni, Lu-Pd, Ni-S, Pd-Ti, Si-Te, Ta-V, and V-Zn. *Journal of Phase Equilibria and Diffusion*, *40*(5), 743-756. https://doi.org/10.1007/s11669-019-00760-w

7. Rogal, L., Bobrowski, P., Körmann, F., Divinski, S., Stein, F., & Grabowski, B. (2017). Computationally-driven engineering of sublattice ordering in a hexagonal AlHfScTiZr high entropy alloy. *Scientific Reports*, *7*(1). https://doi.org/10.1038/s41598-017-02385-w

8. Mende, T., Tatárka, E., Kőrösy, G., & Roósz, A. (2014). Liquidus and Solidus Temperature Calculation in Al-Cu-Fe System by ESTPHAD Method. *Materials Science Forum*, *790-791*, 259-264. https://doi.org/10.4028/www.scientific.net/msf.790-791.259

9. Gryc, K., Smetana, B., Strouhalová, M., Žaludová, M., Michalek, K., Zlá, S., ..., & Dobrovská, J. (2014). Determination of soli-

dus and liquidus temperatures in the low carbon steel using three devices for high-temperature thermal analysis and specialized programs. *MeTal*, (pp. 57-63).
10. Shinde, V. D. (2018). Thermal Analysis of Ductile Iron Casting. *Advanced Casting Technologies*. InTech. https://doi.org/10.5772/intechopen.72030
11. *Lever Rule (Phase Diagrams & Computational Thermodynamics)*. NIST/MML Center for Theoretical and Computational Materials Science/NIST. Retrieved from https://www.ctcms.nist.gov/~kattner/solidifc/lever.html
12. ASM International (2016). *ASM Metals Handbook*. *Volume 03: Alloy Phase Diagrams*. Retrieved from http://www.asminternational.org/search/-/journal_content/56/10192/25871543/PUBLICATION
13. Uzlov, K. I., Repyakh, S. I., Kimstach, T. V., & Karpova, T. P. (2024). Eutectic-peritectic nature of structure formation of copper angle alloys of the Cu-Sn-Al system. *Innovative technologies in science and education. European experience*, (pp. 214-220). Jourfond.
14. Kimstach, T. V., & Uzlov, K. I. (2025). Chemical composition influence on mechanical properties of Cu-Al-Si-Sn-Mn system bronze during its solidification in die mold. *System technologies*, *2*(157), 135-145.

Визначення граничних значень і фазових перетворень інтервалу кристалізації бронзи БрА7К2О1,5Мц0,3

Т. В. Кімстач[1,2], *К. І. Узлов*[1], *О. П. Білий*[1], *Л. І. Солоненко*[3], *С. І. Реп'ях*[*1]

1 – Український державний університет науки і технологій, м. Дніпро, Україна
2 – Інститут чорної металургії імені З. І. Некрасова НАН України, м. Дніпро, Україна
3 – Національний університет «Одеська політехніка», м. Одеса, Україна
[*] Автор-кореспондент e-mail: 123rs@ua.fm

Температури фазових переходів, інтервал кристалізації і т. і. є фундаментальними параметрами будь-якого сплаву. Із ними пов'язані ливарні, технологічні і експлуатаційні властивості сплавів. Тим не менше, на відміну від двокомпонентних бронз, для багатокомпонентної конструкційної, немагнітної, стійкої до корозії бронзи БрА7К2О1,5Мц0,3, такі відсутні.

Мета. Для бронз системи Cu-Al-Si-Sn-Mn встановити кількісні значення показників її інтервалу кристалізації (температури ліквідус і солідус, величину інтервалу кристалізації й відносну долю у ньому твердої фази). Визначити синергетичний і селективний вплив легуючих компонентів бронзи БрА7К2О1,5Мц0,3 на зміну показників її інтервалу кристалізації та відносної рідкоплинності.

Методика. У роботі використані відомі методи й методики досліджень, у числі яких термографування, диференційний термічний аналіз, спектральний хімічний аналіз, метод цифрового аналізу зображень. Рідкоплинність бронз оцінювали на спіральній пробі. Для визначення синергетичного й селективного впливу легуючих елементів бронзи на її показники використали співвідношення в ній хімічних елементів (критерій K_R) і результати обробки експериментальних даних за комп'ютерною програмою Excel.

Результати. У бронзі БрА7К2О1,5Мц0,3 із підвищенням величини критерію K_R з 0,35 до 0,84 зростають температури ліквідус, солідус й інтервал кристалізації з 32 до 49 °С. Визначено синергетичний і селективний вплив легуючих елементів (Al, Si, Sn, Mn) бронзи на її граничні показники інтервалу кристалізації. Встановлено, що умовно-істинні рідкоплинності бронз БрА7К3О1,5Мц0,3 і БрА9Ж3Л практично однакові. Для бронз системи Cu-Al-Si-Sn-Mn із $K_R = 0{,}35–2{,}07$ відносна об'ємна доля твердої фази (φ_T) у температурному інтервалі кристалізації складає 60–63 %.

Наукова новизна. Уперше для бронзи БрА7К2О1,5Мц0,3 визначені граничні значення й фазові перетворення її інтервалу кристалізації, синергетичний і селективний вплив її легуючих елементів на ці показники.

Практична значимість. За обраним хімічним складом бронзи БрА7К2О1,5Мц0,3 запропоновані математичні моделі для розрахунку її температури ліквідус і солідус, переходу із відносних значень залежності об'ємної долі твердої фази (φ_T) у температурному інтервалі кристалізації до абсолютних величин температур $t(\varphi_m)$. Їх використання дозволить підвищити прогнозування точності значень ливарних і технологічних параметрів.

Ключові слова: *бронза, ліквідус, солідус, інтервал кристалізації, рідкоплинність, температура*

The manuscript was submitted 04.03.25.